Turk J Elec Engin, VOL.16, NO.1 2008, © TÜBİTAK

Dual-Band Split-Ring Antenna Design for WLAN Applications

S. Cumhur BAŞARAN[1], **Yunus E. ERDEMLİ**[2]
[1]*Akdeniz University, The Vocational School of Technical Sciences, 07058 Antalya-TURKEY*
e-mail: cbasaran@akdeniz.edu.tr
[2]*Kocaeli University, Electronics and Computer Education Department, 41380 Kocaeli-TURKEY*
e-mail: yunusee@kou.edu.tr

Abstract

A dual-band microstrip antenna based on split-ring elements is introduced for WLAN (2.4/5.2 GHz) applications. The proposed split-ring antenna (SRA) has a compact novel design which provides about 2% impedance-bandwidth without a need for additional matching network. Analysis and design of the proposed microstrip antenna is carried out by means of full-wave simulators based on the finite-element method.

Key Words: *Split-ring, microstrip antenna, dual-band, WLAN, and finite-element method.*

1. Introduction

Compact multi-function antennas play a crucial role in achieving optimum system performance in today's communication networks where multi-band, high speed connectivity with easy access is required. In particular, dual-band operation in 2.4/5.2 GHz bands for wireless local area networks (WLANs) are desired to meet the corresponding IEEE standards, preferably using only one antenna element. In these applications, microstrip antennas are highly utilized due to their compact, planar, lightweight, and low-cost features [1–4].

In this paper, we propose a novel WLAN antenna design based on printed split-ring elements. These elements with inherent μ-negative behavior have recently been used as building blocks of various metamaterial structures, providing highly-resonant frequency responses [5–8]. The proposed split-ring antenna (SRA) with novel configuration consists of split-ring elements and metallic loadings appropriately placed between the rings as shown in Figure 1. The antenna is fed by a current-probe placed in one of the splits in its outer ring. The probe basically represents practical coaxial feeding [9], and in the proposed configuration, there is no additional matching network. The compact SRA design provides dual-band operation for WLAN applications.

The analysis and design of SRA has been carried out using two full-wave simulators based on the finite-element method (FEM), namely the in-house Finite Element Microstrip Antenna Simulator (FEMAS) and the commercially available High Frequency Structure Simulator (HFSS). In the paper, after reviewing the FEM formulation briefly, we present simulation results for the proposed design.

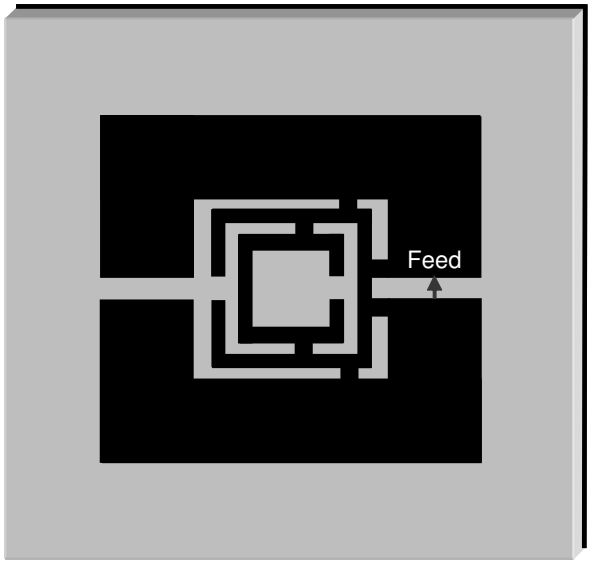

Figure 1. Proposed SRA for WLAN applications (top view is shown).

2. Analysis Method

The FEM is a well-known frequency-domain technique which is highly capable of modeling 3D complex structures with inhomogeneities [10]. In FEM analysis, the structure at hand is first meshed into prism or tetrahedron elements, where unknowns of the problem are usually electric field vector components specified along edges of the elements. The discretized FEM functional is then minimized for each unknown to generate the system matrix, which is mainly sparse. Finally, the FEM system is solved for the edge unknowns via a direct or an iterative solver [10]. In particular, for open (radiation or scattering) problems the computational domain is truncated by an absorbing boundary condition, an artificial absorber or a perfectly-matched layer to simulate the free-space. Alternatively, rather complicated but more accurate truncation can be realized by hybridizing the FEM with the moment method [10].

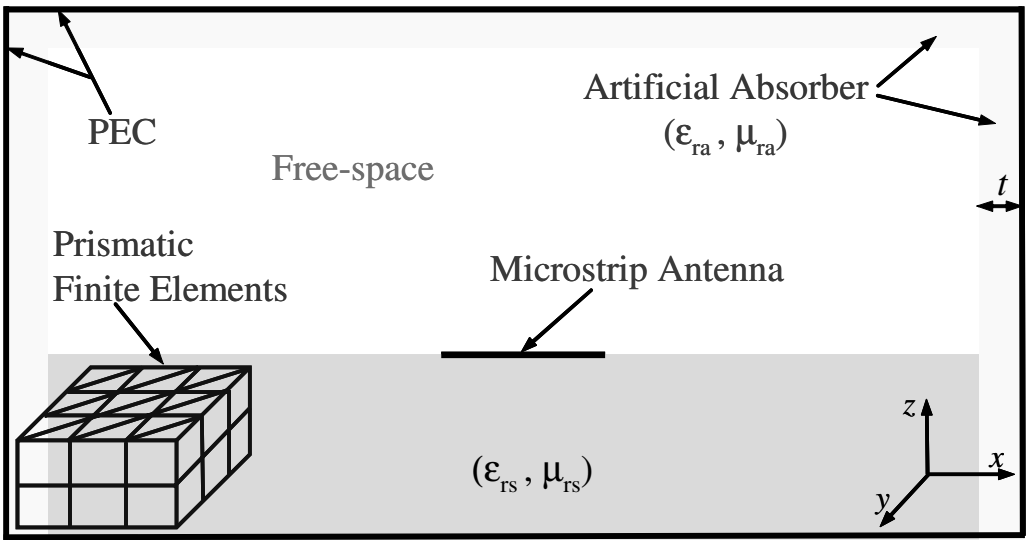

Figure 2. FEM computational domain for a typical microstrip antenna problem (a cross-section view is shown).

In this research, we have developed a FEM-based simulator, named FEMAS. This analysis tool allows 3D modeling of microstrip antennas using uniform prismatic mesh elements and outcomes the corresponding input impedance and pattern characteristics. In particular, the FEMAS has the capability of modeling metallic patches, ideal current-probe feeds, shorting pins, resistive cards, impedance loads (in x, y or z directions) within a metal-backed multilayer dielectric substrate. A cross-section view of the 3D computational domain for a typical microstrip antenna problem is depicted in Figure 2 as an example for FEM modeling employed in the FEMAS. As shown, a microstrip antenna placed over a PEC-backed dielectric substrate with (ε_{rs}, μ_{rs}) radiates to the vacuum-filled upper half-space which is truncated by a PEC-backed artificial absorber with $\varepsilon_{ra} = \mu_{ra} = 1\text{-}j\,2.7$ and thickness $t = 0.15\,\lambda_0$ [11]. For converged field analysis, as the distance (in all directions) between the antenna and the artificial absorber is considered to be minimum value $0.25\,\lambda_0$, each dimension of prismatic finite elements has to be typically smaller than $0.05\,\lambda_0$.

In this study, we have mainly used the commercially available Ansoft HFSS v.10.0 during the design process, particularly due to its speed advantage. The HFSS is also a FEM-based full-wave analysis tool with dissimilar modeling capabilities as compared to the FEMAS. In particular, the HFSS offers non-uniform meshing while uniform gridding is applicable in the FEMAS. In addition, the truncation schemes differ in each simulator. As a result, some discrepancies in the HFSS and FEMAS simulation results are observed.

3. Antenna Design

We now present the details of the design steps that resulted in the proposed WLAN antenna (see Figure 1), noting that a manual optimization scheme was carried out during the design process. A series of parametric studies were carried out to achieve desired antenna performance, particularly tuning the resonant frequencies and impedance levels. In this process, optimized critical antenna parameters were substrate thickness and permittivity (considering the catalogued values), ring dimensions, and positions of the metallic loadings.

We consider the design steps of the WLAN antenna as displayed in Figure 3. The starting configuration (#1) included only one ring element with two splits. While one of the splits was used for the feed placement, the other one was needed to achieve dual-band performance with the inclusion of a secondary split-ring as well as metallic loadings s_1 and s_2 inserted between the rings (#2). The highly resonant impedance characteristics for the configurations #1 and #2 are shown in Figure 4. As can be seen, the inner ring with the loadings s_1 and s_2 provided dual-band profile around 1.9 and 4.2 GHz bands with the impedance levels of 600 Ω and 1100 Ω, respectively. A secondary set of loadings, namely s_3 and s_4, was placed between the rings nearby the feeding gap (#3) so as to decrease those high impedance levels. As shown in Figure 5, the configuration #3 not only resulted in reduced impedance levels ($\sim$30 Ohms), but also shifted the respective frequency bands to 2.2 and 5.1 GHz. Finally, including a third ring (the inner-most) with loadings s_5 / s_6 (#4) provided fine frequency and impedance tuning as seen in Figure 5. Hence, the final configuration #4 allowed for the desired dual-band performance at the designated WLAN bands (2.4/5.2 GHz).

WLAN antenna configuration #4 is re-displayed in Figure 6 with its optimized design parameters. As seen, the SRA composed of three metallic split-rings covers an area of 14 $\times$ 15 mm^2 and placed on a grounded FR4 substrate with 1.6 mm thickness and dielectric constant of 4.4. The outer-most ring with two splits is rather wider than the inner rings with one split each. In addition, each metallic loading inserted appropriately between the ring elements has a size of 0.5 $\times$ 0.5 mm^2.

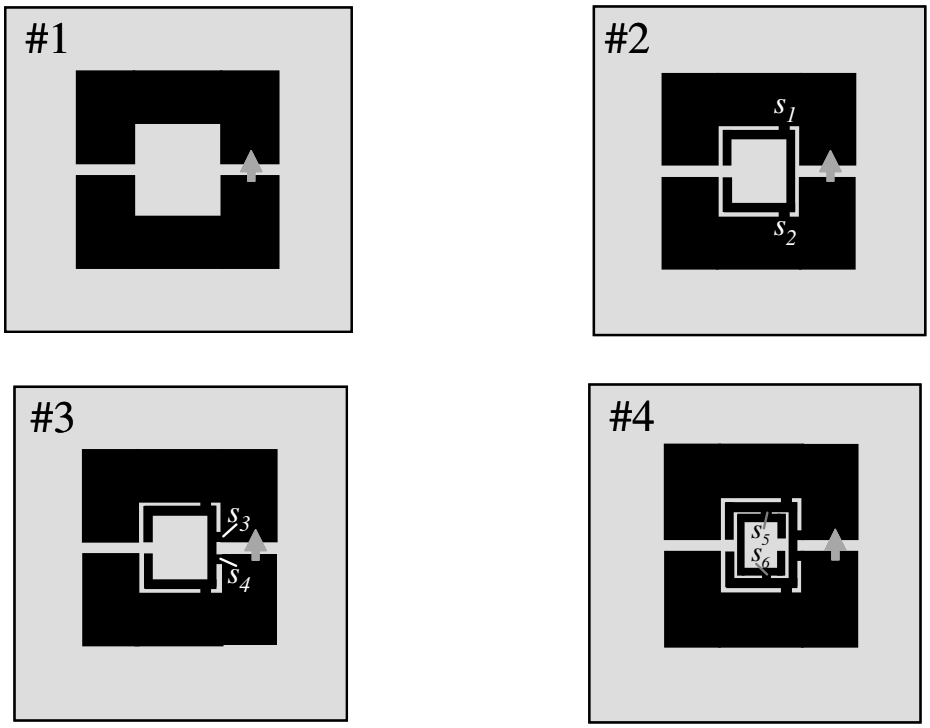

Figure 3. Design steps for the WLAN antenna.

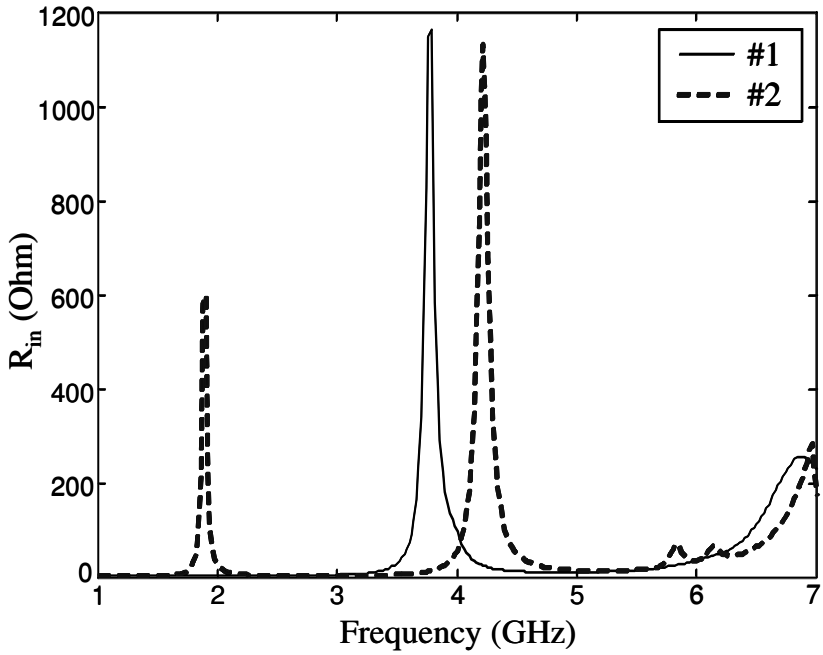

Figure 4. Real parts of the input impedances for the WLAN antenna design configurations #1 and #2.

The input impedance and return loss characteristics of the WLAN–SRA design are displayed in Figures 7 and 8, respectively. As shown, dual-band operation is achieved at 2.43 GHz and 5.23 GHz with corresponding 1.7% and 3.15% bandwidths, respectively; and where the criterion $|S_{11}| < g-10$ dB, with 50 Ω system impedance, is considered. Figure 8 shows the return loss characteristics for both simulators

used in this study, namely the FEMAS and the HFSS. As seen, the simulation results agree with each other relatively well with almost 0.15 GHz frequency shift, which is mainly due to different truncation as well as different meshing schemes employed in each simulator. In addition, radiation patterns of the SRA for the respective frequencies are shown in Figure 9. As seen, E-plane patterns demonstrate desired omni-directional characteristics at each operational frequency. Nevertheless, H-plane patterns show relatively directional behavior. Also, radiation efficiency of the antenna is expected to be almost 50% at 2.4 GHz band and better than 80% at 5.2 GHz band in case of a low-loss dielectric substrate (tan $\delta < 0.01$) as computed data predicts.

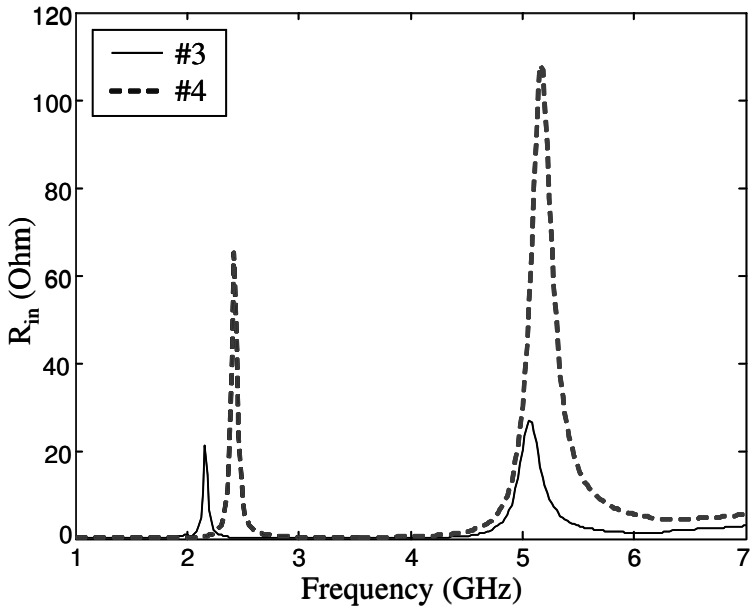

Figure 5. Real parts of the input impedances for the WLAN antenna design configurations #3 and #4.

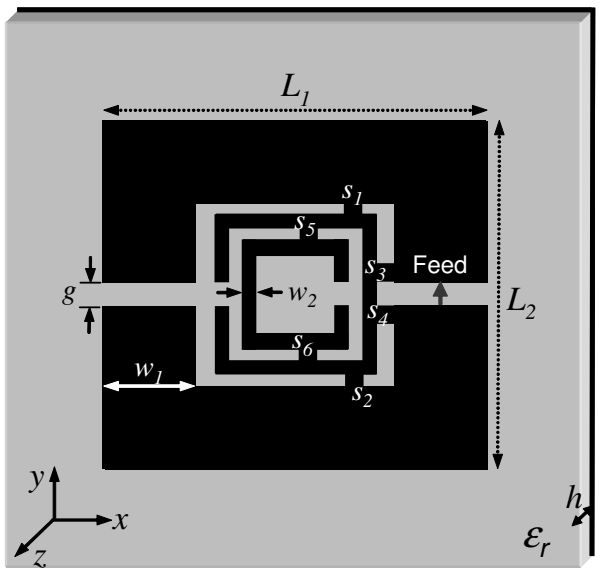

Figure 6. Proposed WLAN–SRA design: $s_1 - s_6$ (metallic loads: 0.5×0.5), $L_1 = 14$, $L_2 = 15$, $w_1 = 4$, $w_2 = 0.5$, $g = 1$, $h = 1.6$ (all in mm), $\varepsilon_r = 4.4$.

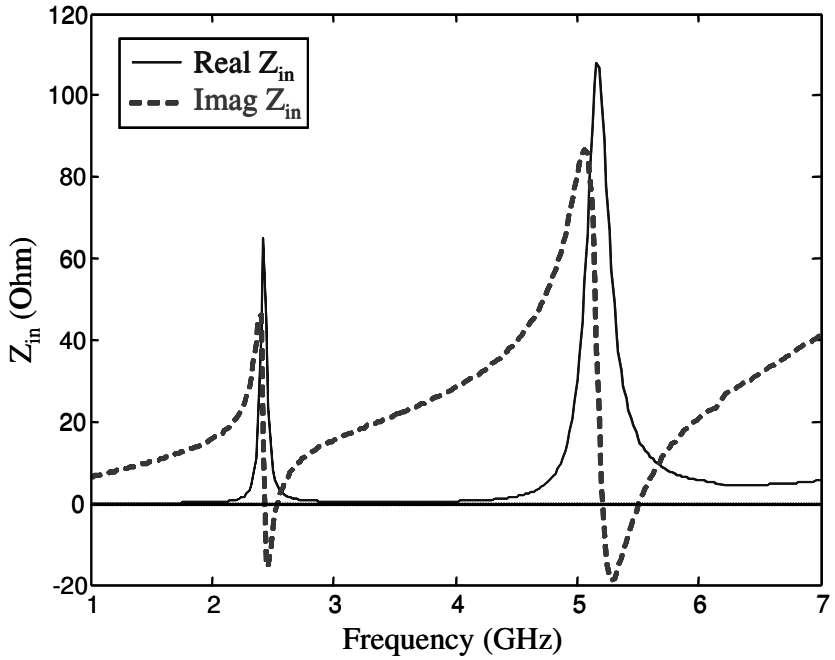

Figure 7. Input impedance (Z_{in}) characteristics of the WLAN–SRA design.

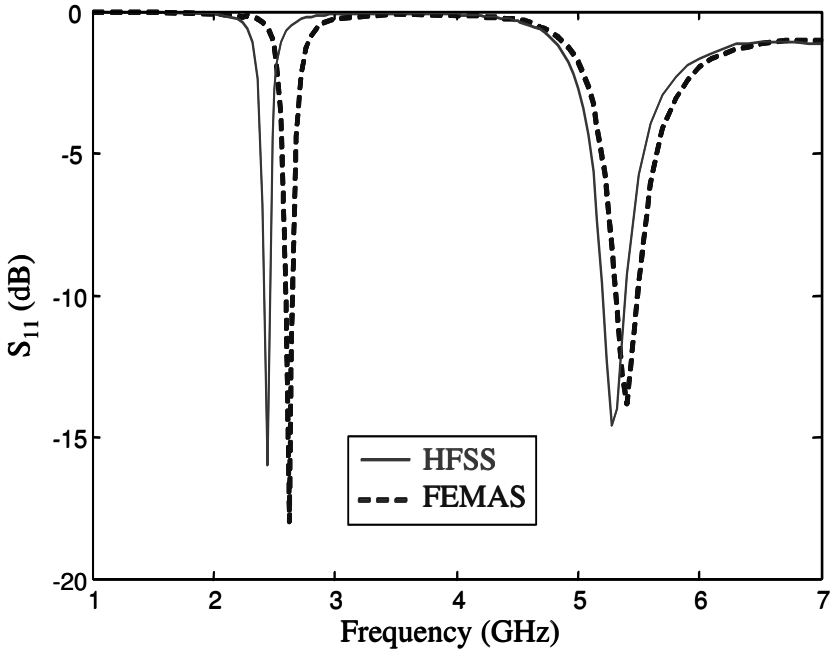

Figure 8. Return loss (S_{11}) characteristics of the WLAN–SRA design.

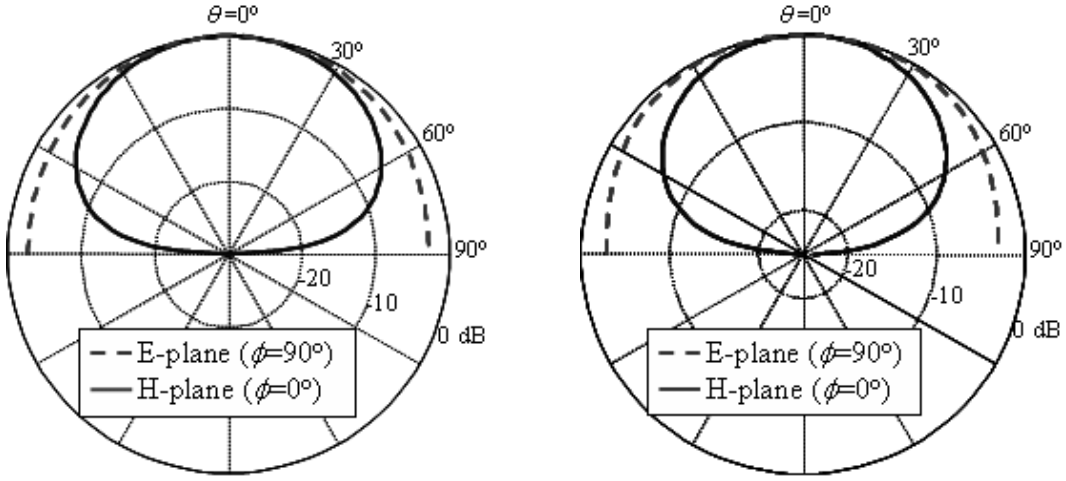

(a) f=2.43 GHz (b) f=5.23 GHz

Figure 9. Radiation patterns of the WLAN–SRA design.

4. Conclusion

In the paper, we have introduced a novel WLAN antenna based on microstrip split-ring elements with metallic loadings. We have presented simulated antenna performances obtained by the well-known HFSS and our in-house FEMAS. In the design, as the outer-most ring is fed by a current-probe, the inner rings with loadings provide frequency-tuning and impedance matching. Thus, the compact SRA design performs dual-band operation at the designated WLAN bands (2.4/5.2 GHz) with almost 2% impedance bandwidth. The operational bands may seem rather narrow mainly due to highly-resonant split-ring elements involved. The bandwidth performance, however, can be improved by means of an additional matching network. Fabrication of the SRA is in progress and measurements will follow.

References

[1] W.J. Liao, Y.C. Lu, H.T. Chou, "A multiband microstrip dipole antenna", IEEE Antennas and Propagation Society International Symposium, Vol. 1A, pp. 462–465, July 3-8, 2005.

[2] H.M. Chen, J.M. Chen, P.S. Cheng, T.F. Lin, "Feed for dual-band printed dipole antenna", Electronics Letters, Vol. 40, No. 21, pp. 1320–1322, Oct. 14, 2004.

[3] H. Rmili, J.M. Floc'h, P. Besnier, M. Drissi, "A dual–band printed dipole antenna for IMT–2000 and 5-GHz WLAN applications", Proceedings of the 9th European Conference on Wireless Technology, Nov. 6–10, 2006.

[4] H.R. Chuang, L.C. Kuo, "3D FDTD design analysis of a 2.4-GHz polarization-diversity printed dipole antenna with integrated balun and polarization-switching circuit for WLAN and wireless communication applications", IEEE Transactions on Microwave Theory and Techniques, Vol. 51, No. 2, pp. 374–381, Feb. 2003.

[5] J.B. Pendry, A.J. Holden, D.J. Robins, W.J. Stewart, "Magnetism from conductors and enhanced nonlinear phenomena", IEEE Transactions on Microwave Theory and Techniques, Vol. 47, No. 11, pp. 2075–2084, Nov. 1999.

[6] D.R. Smith, W.J. Padilla, D.C. Vier, S.C. Nemat-Nasser, S. Schultz, "Composite medium with simultaneously negative permeability and permittivity", Physical Review Letters, Vol. 84, No. 18, pp. 4184–4187, 2000.

[7] Y.E. Erdemli, A. Sondas, "Dual-polarized frequency-tunable composite left-handed slab", Journal of Electromagnetic Waves and Applications, Vol. 19, No. 14, pp. 1907–1918, 2005.

[8] C. Cenk, A. Sondas, Y.E. Erdemli, "Tunable split ring resonator microstrip filter Design", Mediterranean Microwave Symposium, Genova, Italy, Sep. 19–21, 2006.

[9] A.C. Chen, C.L. Tang, Z.H. Lu, "A loop antenna for WLAN application", IEEE Asia-Pacific Conference Proceedings, Vol. 2, Dec. 4–7, 2005.

[10] J.L. Volakis, A. Chatterjee, L.C. Kempel, Finite Element Method for Electromagnetics, IEEE Press & Oxford University Press, New York, 1998.

[11] T. Ozdemir, J.L. Volakis, "A comparative study of an absorber boundary condition and an artificial absorber for truncating finite element mesh", Radio Science, Vol. 29, pp. 1255–1263, September-October, 1994.